

Noise induced stabilization in population dynamics

Matthew Parker,¹ Alex Kamenev,^{1,2} and Baruch Meerson³

¹*School of Physics and Astronomy, University of Minnesota, Minneapolis, MN 55455*

²*William I. Fine Theoretical Physics Institute, University of Minnesota, Minneapolis, MN 55455*

³*Racah Institute of Physics, Hebrew University of Jerusalem, Jerusalem 91904, Israel*

We investigate a model where strong noise in a sub-population creates a metastable state in an otherwise unstable two-population system. The induced metastable state is vortex-like, and its persistence time grows exponentially with the noise strength. A variety of distinct scaling relations are observed depending on the relative strength of the sub-population noises.

The phenomenon of noise induced metastability [1–3] is of importance in ecology [4] and plant biology [5] and has found practical applications in engineering [6]. The typical models [1–3] consider periodically modulated one-dimensional (1d) stochastic systems. The modulation renders the system to be deterministically unstable during a part of the modulation period. An external noise can prevent the escape for several successive periods of external modulation, trapping the system into a metastable state. As a result, the noise causes an increase of the system persistence time by a factor compared to the noiseless case.

Here we consider a different model with two stochastic degrees of freedom, which we call x and y . The y degree of freedom (e.g. imbalance between the numbers of two competing gene alleles) undergoes a strong and fast noise which conserves the total population size x . The latter experiences a slow evolution under the influence of a deterministic potential $V(x)$ along with a sign-definite feedback from the population size imbalance $\propto y^2$ and a relatively weak (demographic) noise. We show that, even if the x -dynamics itself is unstable and prone to a rapid escape, the strong y -noise can lock it in an *exponentially* long-lived vortex-like metastable state. The corresponding exponent exhibits a variety of non-trivial scaling regimes, depending on the relative strength of the noises in the x and y subsystems. A similar model was shown to describe a two-patch Lotka-Volterra system [7]. More distantly related models were recently discussed in the context of biochemical regulatory networks [8] and nanomechanical oscillators [9].

Our model can be cast into the universal form

$$\begin{aligned} \dot{x} &= -V'(x) - y^2 + \xi_x(t), \\ \dot{y} &= -2y + \xi_y(t); \\ \langle \xi_{x(y)}(t) \xi_{x(y)}(t') \rangle &= 2T_{x(y)} \delta(t - t'), \end{aligned} \quad (1)$$

where $V' = dV(x)/dx$, and T_x and T_y characterize the noise strength in the total and differential population size, respectively. The interesting regime of parameters is $T_x < T_y$. The noise effects are substantial when the population is close to a bifurcation point. In this case the properly rescaled deterministic potential takes the form

$$V(x) = -x^3/3 - \delta x, \quad (2)$$

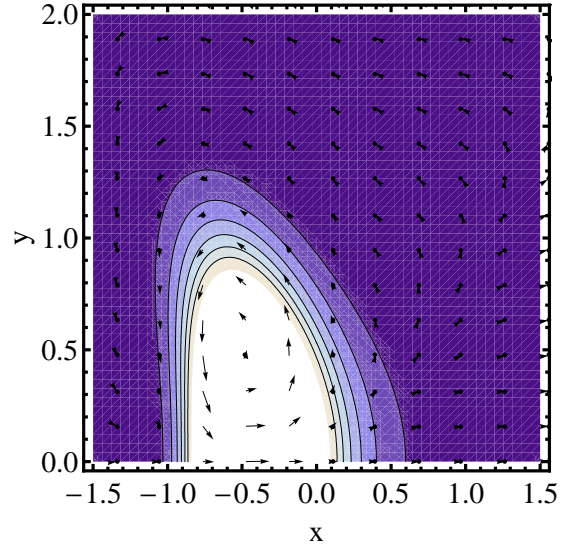


FIG. 1. (Color online) The quasi-stationary FP state. The contours represent the probability density $P(x, y)$; the arrows show the probability current density. The system is symmetric around $y = 0$, and only the top half is shown. $T_x = 0.05$, $T_y = 0.5$.

where δ is the bifurcation parameter, and we have shifted the x variable to have the bifurcation point at $x = 0$.

A simple realization of this model is provided by two species A and B , which undergo the reaction $A + B \xrightarrow{\lambda} 2X$, where X is either A or B . This is the well-known Moran process for modeling neutral genetic drift [10]. This is the fastest process which conserves the total population size. In addition, the population size may slowly evolve according to e.g. the following set of reactions $X \xrightleftharpoons{\beta_{\mp}} 0$ and $A + B \xrightarrow{\alpha} A + B + X$. In this case $x = (n_A + n_B - N)/N$ and $y = (n_A - n_B)/N$, where $N = \beta_-/\alpha$ is the population size close to the bifurcation, and $\delta = 4\alpha\beta_+/\beta_-^2 - 1$ is the bifurcation parameter. In the limit of large population size $N \gg 1$, the corresponding Master equation can be approximated by a Fokker-Planck equation [11]. In the vicinity of the bifurcation

point, the latter reads

$$\begin{aligned} \dot{P}(x, y) = & -\partial_x \left[(-V'(x) - y^2) P(x, y) - \frac{2}{N} \partial_x P(x, y) \right] \\ & - \partial_y \left[-2yP(x, y) - \left(\lambda + \frac{2}{N} \right) \partial_y P(x, y) \right], \end{aligned} \quad (3)$$

where $P(x, y, t)$ is the probability distribution function, and time is measured in units of $2/\beta_-$. Equation (3) is equivalent to the Langevin equations (1), where the two “temperatures” are given by $T_x = 2/N$ and $T_y = T_x + 2\lambda/\beta_-$. When the drift rate λ is fast, one has the strong inequality $T_x \ll T_y$.

First we focus on the case of exact bifurcation, $\delta = 0$. The x -equation takes the form $\dot{x} = x^2 - y^2 + \xi_x$. Without noise the y -variable tends to zero, leading to $\dot{x} = x^2$ dynamics in the x -direction. This has $x = 0$ as the marginally stable point. An arbitrarily weak x -noise is sufficient to kick the system out of this fixed point and set it on the path to unlimited proliferation, $x \rightarrow \infty$. One may think thus that the $\delta = 0$ system is destined to blow up in a very short time. Recall, however, that the y -noise is substantial. Although $\langle y \rangle = 0$, the mean square value $\langle y^2 \rangle > 0$ and is large compared with T_x . One can then expect the x -dynamics to be governed by the effective potential $V_{\text{eff}}(x) = -x^3/3 + \langle y^2 \rangle x$. This potential exhibits a minimum at $x = -\sqrt{\langle y^2 \rangle}$, and a maximum at $x = \sqrt{\langle y^2 \rangle}$. As a result, a long-lived metastable distribution, peaked at $x = -\sqrt{\langle y^2 \rangle}$, can be created. A numerical solution of the Fokker-Planck (FP) equation (3) supports this expectation. Figure 1 shows the slowly varying quasi-stationary distribution observed at late times. Notably, the probability currents develop two counter-rotating vortices. Before reaching the point $x = y = 0$, the “particle” is kicked in the y -direction, where the x -evolution is directed toward population contraction. The vortices, therefore, arrest the population explosion. We note that probability current vortices in non-equilibrium *stationary* states – the Brownian vortices – were recently observed in experiment [12].

Our main goal is to evaluate the lifetime of such a noise-induced vortex-like metastable state. We start from qualitative considerations. As a first approximation one can estimate the mean-square y -deviation in the harmonic potential y^2 , cf. Eq. (1), as $\langle y^2 \rangle = T_y/2$. Therefore $V_{\text{eff}}^{\text{max}} - V_{\text{eff}}^{\text{min}} = \sqrt{2} T_y^{3/2}/3$, and one expects that

$$\ln t_{\text{esc}} \simeq \sqrt{2} T_y^{3/2}/3T_x. \quad (4)$$

Remarkably, the escape time is exponentially *increasing* with the y -noise strength T_y , while exhibiting the standard Arrhenius scaling with T_x . Our numerical simulations of the Langevin Eqs. (1), see Fig. 2, confirm Eq. (4) as long as $T_y^{3/2}/T_x$ is not too large. At larger values of this parameter, however, Eq. (4) greatly overestimates the lifetime of the metastable state.

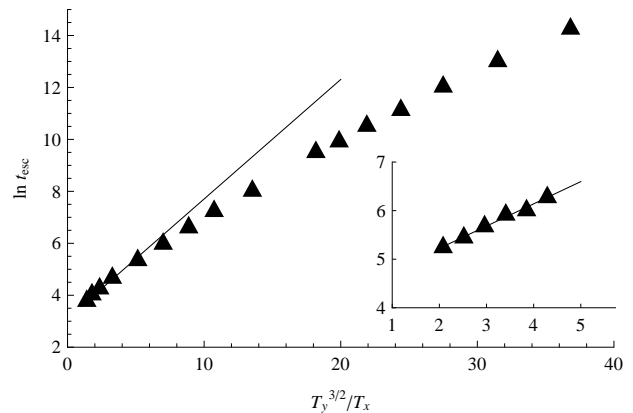


FIG. 2. Simulated escape times for $T_y = 0.05$ and varying T_x . The straight line has slope of $\sqrt{2}/3$, cf. Eq. (4). Inset: the limit $\sqrt{T_x} > T_y$.

The reason for this deviation is that for large T_y the typical potential barrier is too high for the x -motion to overcome. Then, instead of relying on typical realizations of y -noise, the system prefers to wait for a rare y -trajectory which stays anomalously close to $y = 0$. The probability that the y -motion is confined to the interval $|y(t)| < y_0$ for a time t_0 is given by $\exp[-E_y(y_0)t_0]$. Here E_y is the lowest eigenvalue of the 1d FP equation in the y -direction with absorbing boundary conditions at $y = \pm y_0$. E_y can be estimated as $E_y \propto T_y/y_0^2$, where T_y is the proper diffusion coefficient. On the other hand, the probability that during the time interval t_0 the x -coordinate will diffuse from $x = -y_0$ to $x = +y_0$ is given by $\exp(-y_0^2/T_x t_0)$, where T_x is the proper diffusion coefficient. Maximizing the product of these two probabilities with respect to y_0^2/t_0 , one finds that the probability of the optimal rare fluctuation scales as $\exp(-\sqrt{T_y/T_x})$. These estimates suggest that $\ln t_{\text{esc}} \propto \sqrt{T_y/T_x}$ once $\sqrt{T_y/T_x} < T_y^{3/2}/T_x$, i.e. $\sqrt{T_x} < T_y$. This behavior is indeed qualitatively consistent with Fig. 2.

To put these considerations on a more quantitative basis we shall assume that the dynamics can be separated into the fast y -motion and slow x -motion. The latter adiabatically adjusts to the instantaneous value of $y^2(t)$. We then solve an auxiliary problem of finding the probability of y -trajectories with a given functional form $\langle y^2 \rangle = y_0^2(t)$. Here $y_0(t)$ is an arbitrary *slow* function of time, such that $y_0(\pm\infty) = \sqrt{T_y/2}$, while the averaging is taken over the fast y -fluctuations. Integrating over an intermediate time-scale Δt that is long relative to these fluctuations one can then write $\int_{t-\Delta t}^{t+\Delta t} [y_0^2(t) - y^2(t)] dt = 0$. We can thus introduce the functional constraint $\delta(\int [y^2(t) - y_0^2(t)] dt)$ into the stochastic functional integral over $\mathcal{D}y$ [13–15] and elevate it into the exponent with the help of the auxiliary *slow*

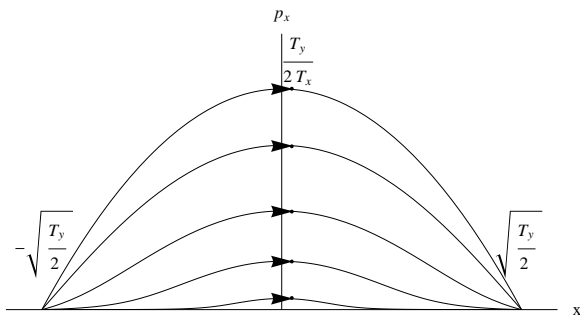


FIG. 3. Phase portrait of the optimal escape paths for different T_x . Lower lines correspond to lower values of T_x . The momentum has been rescaled by T_y/T_x so that all paths would coincide if they followed simple activation [assumed by Eq. (4)].

field $\chi(t)$. As a result we obtain an effective Lagrangian

$$\mathcal{L}_y = \frac{(\dot{y} + 2y)^2}{4T_y} - \chi(y^2 - y_0^2), \quad (5)$$

where the χ -integration runs from $-i\infty$ to $i\infty$. Employing the slowness of the $\chi(t)$ field, the Gaussian integral over the fast $y(t)$ can be evaluated using the Fourier transformation. This leads to an effective Lagrangian for χ in the form

$$\mathcal{L}_\chi = \chi y_0^2 - \int \frac{d\omega}{2\pi} \ln \left(1 + \frac{4T_y \chi}{\omega^2 + 4} \right) = \chi y_0^2 + 1 - \sqrt{T_y \chi + 1}. \quad (6)$$

Finally, the χ -integration can be evaluated in the saddle point approximation: $\chi(t) = T_y/4y_0^4 - T_y^{-1}$. This yields the probability of y -motion conditioned on $\langle y^2 \rangle = y_0^2(t)$:

$$P[y_0] \propto e^{-\int dt E_y(y_0)}, \quad E_y(y_0) = \frac{T_y}{4y_0^2} - 1 + \frac{y_0^2}{T_y}. \quad (7)$$

Notice that E_y is non-negative and equal to zero if and only if $y_0^2 = T_y/2$. Therefore, the condition $y_0^2(\pm\infty) = T_y/2$ is necessary for convergence of the integral in Eq. (7). The saddle point calculation is justified as long as $\int dt E_y[y_0(t)] \gg 1$.

Having found the conditional probability of y -motion with a given profile of $\langle y^2 \rangle$, we turn now to the x -degree of freedom. According to the scale separation assumption, it is governed by the Langevin equation $\dot{x} = x^2 - y_0^2(t) + \xi_x(t)$, where $y_0^2(t)$ is a slow function of time with $y_0^2(\pm\infty) = T_y/2$ and $y_0^2(0) < T_y/2$. Our goal is to evaluate the escape rate of the x -variable from its metastable minimum at $x = -\sqrt{T_y/2}$ during the time when $y_0^2(t)$ is suppressed with respect to its asymptotic values. We then maximize this escape rate, taken with weight $P[y_0]$, Eq. (7), against the optimal time-dependent variance $y_0(t)$.

Since the escape rate in the x -direction is expected to be small, it can be found through a semiclassical treat-

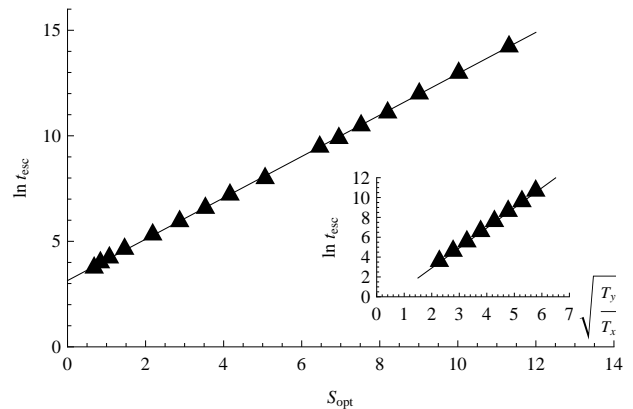


FIG. 4. Simulated escape times vs. the optimal action for $T_y = 0.05$ and varying T_x . Inset: the limit $(T_y^2/T_x)^{1/6} \gg 1$ (with $T_y = 1000$). The straight line is Eq. (11).

ment of the corresponding FP equation [16]. The proper FP Hamiltonian has the form

$$\mathcal{H}[x, p_x; y_0(t)] = p_x[-V'(x) - y_0^2 + T_x p_x] - E_y[y_0(t)], \quad (8)$$

where x and p_x are canonically conjugate variables, and $y_0(t)$ is an external time-dependent parameter. The last term accounts for the statistical weight of a realization of $y_0(t)$, given by $P[y_0]$, Eq. (7). If $y_0(t)$ is an adiabatically slow function, the escape proceeds along the zero-energy trajectory of this Hamiltonian, which connects the two fixed points $(-\sqrt{T_y/2}, 0)$ and $(+\sqrt{T_y/2}, 0)$ on its (x, p_x) phase plane, Fig. 3. Putting $V(x) = -x^3/3$, one finds for the (slowly varying in time) optimal trajectory

$$p_x(x; y_0) = \frac{1}{2T_x} \left[y_0^2 - x^2 + \sqrt{(y_0^2 - x^2)^2 + 4T_x E_y(y_0)} \right]. \quad (9)$$

The corresponding escape time, within exponential accuracy, is given by the classical action, i.e. the area of the phase plane under the zero-energy trajectory

$$\ln t_{\text{esc}}[y_0] = S[y_0] = \int_{-\sqrt{T_y/2}}^{\sqrt{T_y/2}} p_x(x; y_0) dx. \quad (10)$$

The final step is to find the optimal y_0 realization. This is achieved by demanding $\delta S[y_0]/\delta y_0 = 0$, solving for an implicit function of time $y_0 = y_0(x)$ and substituting it back into Eq. (10). This leads to the optimal action, S_{opt} , and corresponding escape time $\ln t_{\text{esc}} = S_{\text{opt}}$. In Fig. 4 this escape time is compared with our Monte-Carlo simulations results, and an excellent agreement is observed.

It is easy to show that, for $T_y \ll \sqrt{T_x}$, the optimal y_0 tends to $\sqrt{T_y/2}$ and thus $E_y \rightarrow 0$, while $S_{\text{opt}} = \sqrt{2} T_y^{3/2}/3T_x$. We thus recover Eq. (4). In the opposite limit $T_y \gg \sqrt{T_x}$, one finds $y_0(0) \ll \sqrt{T_y/2}$. One can thus simplify Eq. (7) as $E_y \approx T_y/4y_0^2$. With this

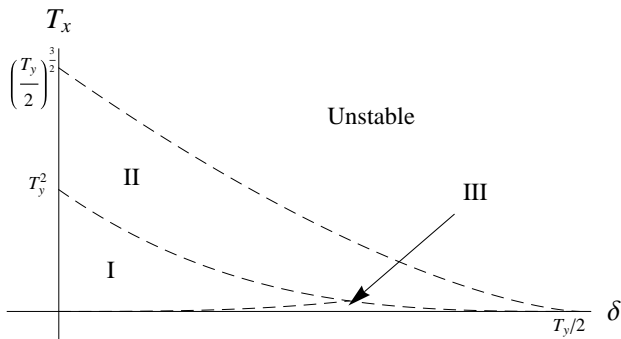


FIG. 5. Phase diagram of the system as a function of T_x and δ with T_y held constant. The dashed lines represent crossovers between different scaling relations. In region I, $\ln t_{\text{esc}} = 2\pi/3\sqrt{T_y/T_x}$. In region II, $\ln t_{\text{esc}} = 4(T_y/2 - \delta)^{3/2}/3T_x$. In region III, $\ln t_{\text{esc}} = \pi T_y/2\delta^{3/2}$.

substitution Eq. (9) can be simplified by the rescaling $x = \tilde{x}(T_x T_y)^{1/6}$ and $y_0 = \tilde{y}_0(T_x T_y)^{1/6}$, which brings the action (10) into the form $S = \sqrt{T_y/T_x} \int \tilde{p}(\tilde{x}; \tilde{y}_0) d\tilde{x}$. The integration limits are $\pm(T_y^2/T_x)^{1/6} \rightarrow \pm\infty$ in the limit of interest, while $\tilde{p} = \left[\tilde{y}_0^2 - \tilde{x}^2 + \sqrt{(\tilde{y}_0^2 - \tilde{x}^2)^2 + \tilde{y}_0^{-2}} \right] / 2$ is a parameterless function. Optimizing it over \tilde{y}_0 and performing \tilde{x} -integration, one finds

$$\ln t_{\text{esc}} = \frac{2\pi}{3} \sqrt{\frac{T_y}{T_x}}, \quad \sqrt{T_x} \ll T_y, \quad (11)$$

which confirms our qualitative estimates below Eq. (4) and provides the numerical factor. The latter is compared with our Monte-Carlo simulations in the inset of Fig. 4. Notice that the actual condition for the applicability of the asymptotic result (11) is $1 \ll (T_y^2/T_x)^{1/6}$. Again, the population lifetime *increases* with the y -noise strength. Notice also that the normal Arrhenius scaling in the parameter T_x gives way to a stretched exponential law with $T_x^{-1/2}$. A similar transition is known as Efros-Shklovskii law [17] in the context of hopping transport in disordered semiconductors.

We consider now deviations from the exact bifurcation point, i.e. $\delta \neq 0$. If $|\delta| \gg T_y$, the deterministic “force”, cf. Eq. (2), is very strong, and the y -noise is not important for the system’s persistence time. At $\delta = \delta_c = T_y/2$ the effective force associated with the y -noise is canceled by the deterministic δ -force. This causes a noise-induced shift in the bifurcation of the x -dynamics. That is, it is much harder to destabilize the population in the presence of strong y noise. In the vicinity of this noise-shifted bifurcation one finds the standard scaling of the lifetime $\ln t_{\text{esc}} = 4(\delta_c - \delta)^{3/2}/3T_x$, cf. Eq (4).

On the other hand, away from the the noise-shifted bifurcation, i.e. at $|\delta - \delta_c|/\delta_c > (\sqrt{T_x}/T_y)^{2/3}$, the scaling changes qualitatively. To find the new scaling we look for the zero energy trajectory of the Hamiltonian (8) with

$\delta \neq 0$ and $E_y = T_y/4y_0^2$ and optimize the action over $y_0(x)$, as explained above. In this way we find

$$\ln t_{\text{esc}} = \frac{2\pi}{3} \sqrt{\frac{T_y}{T_x}} \mathcal{S} \left[\frac{\delta}{(T_x T_y)^{1/3}} \right], \quad \sqrt{T_x} \ll T_y, \quad (12)$$

where the universal function $\mathcal{S}(\tilde{\delta})$ has the following asymptotic limits: $\mathcal{S}(\tilde{\delta}) \approx 1 + 0.71\tilde{\delta}$ for $\tilde{\delta} \ll 1$ and $\mathcal{S}(\tilde{\delta}) \approx 3\tilde{\delta}^{-3/2}/4$ for $\tilde{\delta} \gg 1$. This means that the scaling of the population lifetime given by Eq. (11) is basically intact as long as $\delta \lesssim (T_x T_y)^{1/3}$. In the opposite limit, the escape time scales as

$$\ln t_{\text{esc}} = \pi T_y/2\delta^{3/2}. \quad (13)$$

This is independent of T_x . For $\delta > (T_x T_y)^{1/3}$ the system can escape even at $T_x = 0$ via paths with unusually small y . Figure 5 shows the regions where the three scaling relations (4), (11), (13) are valid.

In summary, we have studied a novel system where strong noise creates metastability. Increasing the noise strength T_y increases the lifetime of the (vortex-like) metastable state. Escape from this state is governed by a variety of scaling relations depending on the relative role of T_x (the strength of noise in the total population size) and T_y (the strength of noise in the differential size).

We are grateful to J. Krug and M. Dykman for valuable discussions. This research was supported by NSF Grant DMR-0804266 and U.S.-Israel Binational Science Foundation Grant 2008075.

-
- [1] I. Dayan, M. Gitterman, and G. Weiss, Phys. Rev. A, **46**, 757 (1992).
 - [2] R. Mantegna and B. Spagnolo, Phys. Rev. Lett., **76**, 563 (1996); A. Fiasconaro and B. Spagnolo, Phys. Rev. E, **80**, 041110 (2009).
 - [3] A. Mielke, Phys. Rev. Lett., **84**, 818 (2000).
 - [4] V. Guttal and C. Jayaprakash, Ecol. Modell., **201**, 420 (2007).
 - [5] P. D’Odorico, F. Laio, and L. Ridolfi, Proc. Natl. Acad. Sci. USA, **102**, 10819 (2005).
 - [6] R. Ibrahim, J. Vib. Control, **12**, 1093 (2006).
 - [7] R. Abta, M. Schiffer, and N. Shnerb, Phys. Rev. Lett., **98**, 98104 (2007).
 - [8] M. Assaf and B. Meerson, Phys. Rev. Lett., **100**, 58105 (2008).
 - [9] J. Atalaya, A. Isacson, and M. Dykman, arXiv:1103.2758.
 - [10] P. Moran, *The Statistical Processes of Evolutionary Theory* (Clarendon Press, Oxford, 1962).
 - [11] N. van Kampen, *Stochastic Processes in Physics and Chemistry* (North Holland, Amsterdam, 1992).
 - [12] B. Sun, J. Lin, E. Darby, A. Grosberg, and D. Grier, Phys. Rev. E, **80**, 010401(R) (2009).
 - [13] P. Martin, E. Siggia, and H. Rose, Phys. Rev. A, **8**, 423 (1973).
 - [14] C. de Dominicis, J. Physique (Paris), **37**, 1 (1976).

- [15] H. Janssen, *Z. Physik B.*, **23**, 377 (1976).
- [16] M. Freidlin and A. Wentzell, *Random Perturbations of Dynamical Systems* (Springer-Verlag, Berlin, 1984); M. Dykman and M. Krivoglaz, "Physics Reviews", **5**, 266 (1984); R. Graham, in "Theory of Continuous Fokker-Planck Systems", edited by F. Moss and P. McClintock (Cambridge University Press, Cambridge, 1989) Chap. 7, p. 225.
- [17] B. Shklovskii and A. Efros, *Electronic Properties of Doped Semiconductors*, Vol. 1 (Springer-Verlag, Berlin, 1984).